Published in final edited form as:
J Hepatol. 2014 May ; 60(5): 1032–1039. doi:10.1016/j.jhep.2013.12.022.

MMP-9 DEFICIENCY SHELTERS ENDOTHELIAL PECAM-1 EXPRESSION AND ENHANCES REGENERATION OF STEATOTIC LIVERS AFTER ISCHEMIA AND REPERFUSION INJURY

Hiroyuki Kato[1], **Naohisa Kuriyama**[1], **Sergio Duarte**[1], **Pierre-Alain Clavien**[2], **Ronald W. Busuttil**[1], and **Ana J. Coito**[1,*]

[1]The Dumont-UCLA Transplant Center, Division of Liver and Pancreas Transplantation, Department of Surgery, David Geffen School of Medicine at UCLA, Los Angeles, CA [2]Swiss HPB (Hepato-Pancreato-Biliary) Center, Department of Surgery, University Hospital Zurich, 100 Raemistrasse, 8091 Zurich, Switzerland

Abstract

Background & Aims: Organ shortage has led to the use of steatotic livers in transplantation, despite their elevated susceptibility to ischemia/reperfusion injury (IRI). Matrix metalloproteinase-9 (MMP-9), an inducible gelatinase, is emerging as a central mediator of leukocyte traffic into inflamed tissues. However, its role in steatotic hepatic IRI has yet to be demonstrated.

Methods: We examined the function of MMP-9 in mice fed with a high-fat diet (HFD), which developed approximately 50% hepatic steatosis, predominantly macrovesicular, prior to partial hepatic IRI.

Results: The inability of MMP-9−/− deficient steatotic mice to express MMP-9 significantly protected these mice from liver IRI. Compared to fatty controls, MMP-9−/− steatotic livers showed significantly reduced leukocyte infiltration, proinflammatory cytokine expression, and liver necrosis. Loss of MMP-9 activity preserved platelet endothelial cell adhesion molecule-1 (PECAM-1) expression, a modulator of vascular integrity at the endothelial cell–cell junctions in steatotic livers after IRI. Using *in vitro* approaches, we show that targeted inhibition of MMP-9 sheltered the extracellular portion of PECAM-1 from proteolytic processing, and disrupted leukocyte migration across this junctional molecule. Moreover, the evaluation of distinct parameters of regeneration, proliferating cell nuclear antigen (PCNA) and histone H3 phosphorylation (pH3), provided evidence that hepatocyte progression into S phase and mitosis was notably enhanced in MMP-9−/− steatotic livers after IRI.

[*]**Contact Information:** Ana J. Coito, The Dumont-UCLA Transplant Center, 77-120 CHS, Box: 957054, Los Angeles, CA 90095-7054. acoito@mednet.ucla.edu.

Conflict of interests: None

Conclusion: MMP-9 activity disrupts vascular integrity at least partially through a PECAM-1 dependent mechanism and interferes with regeneration of steatotic livers after IRI. Our novel findings establish MMP-9 as an important mediator of steatotic liver IRI.

Keywords

MMP-9; PECAM-1; hepatic steatosis; liver ischemia reperfusion injury

Hepatic ischemia and reperfusion injury (IRI) remains a major clinical limitation in orthotopic liver transplantation.[1] Steatosis, characterized by the deposition of triglyceride-rich lipid droplets in the cytoplasm of hepatocytes,[2] affects approximately 30% of potential donors for liver transplantation.[3] The shortage of organ donors has led to the use of steatotic livers in transplantation, which have increased susceptibility to IRI.[3] The presence of moderate to severe hepatic steatosis (>30%) results in significantly elevated rates of primary nonfunction,[4] and decreased graft and patient survival.[5] Moreover, livers with macrovesicular fat deposition have lower tolerance to IRI when compared to microsteatotic livers.[6] Along with transplantation, steatosis has negative impact in other clinical situations, such as hepatectomy, shock, and cardiac arrest, which are all subject to warm hepatic IRI.

Leukocyte migration with subsequent release of cytokines and free radicals has well documented deleterious effects in hepatic IRI.[1] The recruitment of leukocytes across endothelium is a complex process dependent on cellular adhesion-release and focal matrix degradation mechanisms.[7] While newly synthesized adhesion molecules provide leukocyte attachment to the vascular endothelium, matrix metalloproteinases (MMPs) facilitate their movement across vascular barriers. Among the different MMPs, MMP-9, an inducible enzyme expressed primarily by leukocytes, has been growingly recognized in pathologies that require disruption of basement membranes, multiple sclerosis,[8] postoperative ileus,[9] kidney IRI,[10] islet transplantation,[11] and acute small-for-size liver graft Injury.[12]

We have previously shown that MMP-9 expression/activity is highly detected in steatotic liver transplants,[13] and that MMP-9 mediates leukocyte migration after liver IRI in lean mice.[14] To unveil its function in steatotic IRI, we fed MMP-9−/− deficient mice and MMP-9+/+ wild-type littermates with a steatosis-inducing diet prior to 60 minutes of hepatic ischemia followed by reperfusion.

MATERIALS AND METHODS

Animals, Diet, and Model of Hepatic IRI

Mice were either obtained directly from The Jackson Laboratory or from its derived breeders in our UCLA facility. C57BL6 mice were fed a high-fat diet (HFD; 60% kcal in fat; Research Diets, D12492), or normal chow, from either 4 or 7 to 12 weeks of age. MMP-9-deficient (MMP-9−/−) knockout (KO) mice (FVB.Cg-Mmp9tm1tvu) and matched MMP-9+/+ wild-type (WT) littermates were fed a HFD diet from 4 to 12 weeks of age. Twelve-week-old male mice were subjected to hepatic IRI, as published.[14] Briefly, arterial and portal venous blood supplies were interrupted to the cephalad lobes of the liver

for 60 minutes using an atraumatic clip, and mice were sacrificed after reperfusion. All animals received humane care according to the criteria outlined in the Guide for the Care and Use of Laboratory Animals published by the National Institutes of Health.

Serum Transaminases

Serum alanine transaminase (ALT) and serum aspartate transaminase (AST) levels were measured using a commercially available kit (Teco Diagnostics, Anaheim, CA), following manufacturer's instructions.

Tissue Triglyceride Levels

Liver triglyceride contents were carried out using the LabAssayTM Triglyceride Kit (Wako Pure Chemical Industries Ltd., Osaka, Japan), following manufacturer's instructions.

Histology and Immunohistochemistry

Liver histology and immunohistochemistry were performed as previously published.[14, 15] Liver specimens embedded in paraffin were processed for hematoxylin and eosin (H&E) staining. Liver steatosis was assessed by Oil Red O staining. Immunohistochemistry was performed using CD3 (HIT3a), Ly-6G (1A8), and PECAM-1 (MEC13.3) from BD Biosciences, CD68 (FA-11, Serotec), MMP-9 (AF909; R&D Systems), vWF (A0082, DAKO), PCNA (PC10; Neomarkers) and pH3 (Ser10; Cell Signaling) antibodies at optimal dilutions. Dual/triple staining was detected by immunofluorescence with Alexa Fluor 594 (red) and Alexa Fluor 488 (green) labeled secondary antibodies (Molecular Probes). Alexa Fluor 488 phalloidin and Vectashield mounting media with DAPI (Vector Laboratories) were used for F-actin and nuclear staining, respectively. Sections were blindly evaluated by counting 10 high-powered fields (HPFs)/section in triplicate. The proliferation index is expressed as the percentage of PCNA, or pH3 stained hepatocytes per total number of hepatocytes.

Western blot and Zymography Analysis

Western blots and Zymography were performed as described.[14] PVDF membranes were incubated with antibodies against PECAM-1 (epitope within extracellular domain; SC-28188; Santa Cruz), His-Tag (27E8; Cell Signaling), PCNA (PC-10), and pH3 (Ser10). After development, membranes were stripped and reblotted with anti-actin antibody (Santa Cruz). Gelatinolytic activity was assessed in liver extracts and culture supernatants on 10% SDS-PAGE gels contained 1 mg/mL of gelatin under nonreducing conditions. Prestained molecular weight markers (Bio-Rad) and MMP-9 (BIOMOL) served as standards. Relative quantities of protein were determined using a densitometer (NIH Image J software).

IL-6 Protein Expression

Serum IL-6 protein content was determined using a commercially available ELISA kit (eBioscience, San Diego, CA) following manufacturer's instructions, with final results expressed in picograms of IL-6 per milliliter of serum.

RNA Extraction and Reverse Transcriptase PCR

RNA was extracted from livers with Trizol (Life Technologies) as described.[14] Reverse transcription was performed using 5 μg of total RNA in a first-strandcDNA synthesisreaction with SuperScript III RNaseH Reverse Transcriptase (LifeTechnologies). The cDNA product was amplified by PCR using primers specific for each target cDNA.

Cell Culture

Bone marrow–derived neutrophils were isolated from MMP-9−/− and WT-MMP-9+/+ mice as previously published.[14] The bone marrow preparations were resuspended at 5×10^7 cells/mL in HBSS and the cells were layered on Percoll gradients (Sigma-Aldrich). Mature neutrophils were >90% pure and >95% viable in the neutrophil-rich fractions. Isolated neutrophils were stimulated with formyl-Met-Leu-Phe-OH (fMLP; 50 nM; Calbiochem). After 12h of conditioning, medium was recovered and concentrated using microcon centrifugal filter units (Amicon Microcon UFC40SV, Millipore). The recombinant PECAM-1 containing a 6×His tag on its C terminus (rPECAM-1-100kDa; 500ng; R&D systems) was then incubated with PBS or with neutrophil-conditioning medium with or without different doses of MMP-9 inhibitor-I (100-200nM; C27H33N3O5S; Calbiochem).

In Vitro Migration Assay

Bone marrow–derived neutrophils and thioglycollate-elicited peritoneal macrophages were purified as previously published.[14, 16] Isolated neutrophils and macrophages were resuspended in RPMI-1640 without FBS and transmigration through either PECAM or an endothelial cell monolayer was performed using a commercially available *in vitro* cell migration assay kit (BD Bioscience). Briefly, 6.5-mm-diameter Transwell inserts with 3-μm pores were coated with either rPECAM (500ng/well; R&D systems), human umbilical vein endothelial cells (HUVECs), grown as monolayer [17], or remained uncoated (control invasion chambers) on 24-well culture trays. Neutrophils or macrophages were added at 5×10^5 cells/well to the top chamber with or without different doses (100 and 200nM) of MMP-9 inhibitor-I; CXCL-8 (100ng/ml; neutrophil migration) and TNF-α (10ng/ml; macrophage migration) were added to the lower chamber. Neutrophils and macrophages were incubated at 37°C and 5% CO2 for 4h and 6h, respectively, and the cells that had migrated into the lower chamber were collected, stained, and counted as previously reported. [14, 16]

Data Analysis

Results are expressed as mean ± standard deviation. Statistical comparisons between groups of normally distributed data were performed with the Student t test using the statistical package SPSS (SPSS Inc., Chicago, IL). P values less than 0.05 were considered statistically significant.

RESULTS

HFD-fed C57BL6 Mice Developed Macrosteatosis and Exacerbated Hepatic IRI

HFD-fed C57BL6 mice develop fatty livers resembling human obesity.[18] In our settings, body weight and liver weight were significantly higher in 8-week HFD-fed mice, compared with 5-week HFD mice ($p<0.05$) and lean animals ($p<0.05$) (Supplementary Fig. 1 A-C). Liver triglyceride levels were markedly elevated in 8-week HFD-fed mice (113.8±20.1 μg/mg liver), compared with 5-week HFD-fed (21.7±4.1 μg/mg liver; $p<0.05$) and lean (10.8±1.2 μg/mg liver; $p<0.05$) animals (Supplementary Fig.1D). Moreover, 8-week HFD-fed mice were characterized by ~50% liver steatosis, with macrovesicular fatty (MaS) infiltration, as assessed by Oil Red-O staining (Supplementary Fig. 1E). Conversely, 5-weeks HFD-fed animals showed mainly microsteatosis (MiS), and lean mice had virtually no liver fat inclusions. Further, the serum AST and ALT levels (U/l) were significantly elevated in animals with MaS livers compared with MiS ($p<0.05$) and lean ($p<0.05$) mice after IRI (Supplementary Fig. 2A and B). The elevated aminotransaminase levels in the 8-week HFD-fed mice correlated with increased necrosis and MMP-9 activity in the fatty livers post-IRI (Supplementary Fig 2C-E).

HFD-fed MMP-9−/− and MMP-9+/+ Mice Developed Comparable Liver Steatosis

MMP-9−/− deficient mice and respective MMP-9 +/+ wild-type control littermates fed with the high fat diet (HFD) for eight weeks developed comparable body weight, liver weight, and liver/body weight ratios (Table 1). MMP-9−/− and MMP-9+/+ livers also showed similar levels of triglycerides (97.8±16 versus 99.9±23 μg/mg liver) and fat deposition (≈50%), with macrovesicular fatty infiltration, after the feeding period (Table 1). These data, therefore, establish that MMP-9 deficiency did not interfere with the development of hepatic macrovesicular steatosis in HFD-fed mice.

Characterization of MMP-9 Deficiency in Steatotic Mouse Livers

MMP-9 expression/activity was virtually absent in naive MMP-9−/− and MMP-9+/+ steatotic livers; however, it was highly expressed, predominantly by infiltrating leukocytes, in wild-type MaS control livers post-IRI. MMP-9 was undetectable in MMP-9-deficient MaS livers post-reperfusion (Supplementary Fig. 3).

MMP-9 Deficiency Improved Steatotic Liver Function and Histology after IRI

We used 8-week HFD fed mice, which developed ~50% hepatic steatosis, predominantly macrovesicular, to examine whether lack of MMP-9 activity confers protection against marginal hepatic IRI. MaS-MMP-9−/− mice showed significantly ($p<0.05$) reduced serum aminotransaminase levels (U/L) at 6h (AST: 2,638±1,115 versus 8,750± 2,528; ALT: 2,825± 2,115 versus 11,461± 4,293), 24h (AST: 3,532±1,846 versus 7,906± 2,011; ALT: 1,853±1,302 versus 3,841±1,950) and 48h (ALT: 172±49 versus 534±121) after IRI (Fig. 1). MaS-MMP-9−/− livers were characterized by decreased sinusoidal congestion and reduced percentage of liver necrosis after reperfusion, compared to the highly damaged fatty controls (Fig. 1).

MMP-9 Deficiency Depressed Leukocyte Infiltration and Activation in Steatotic Liver IRI

Ly-6G neutrophil (6h: 29±11 versus 66±18; 24h: 94±67 versus 248±35; $p<0.05$), CD68 macrophage (6h: 53.3±6.1 versus 81.6±16.9; 24h: 72.7±10.6 versus 132.0±27.3; $p<0.05$) and CD3 lymphocyte (6h: 19.8±7.02 versus 36.6 ±6.5; 24h: 25.3±10.8 versus 47.7±7.0; $p<0.05$) infiltration was clearly depressed in the portal areas of MaS-MMP-9−/− livers post-IRI (Fig. 2A, and B). The mRNA expression (cytokine/β actin ratio) of IL-6 (6h: 0.09±0.12 versus 0.55±0.31; 24h: 0.14±0.07 versus 0.38±0.07; $p<0.05$), IFN-γ (24h: 0.11±0.05 versus 0.39±0.12; $p<0.05$), and TNF-α (24h: 0.59±0.16 versus 0.86±0.09; $p<0.05$), was significantly depressed in MaS-MMP-9−/− livers post-reperfusion. Furthermore, IL-6 protein levels (pg/ml) were markedly decreased in the serum of MaS-MMP-9−/− mice at 6h (77.3±10.7 versus 307.3±132.2; $p<0.05$) and 24h (14.6±3.0 versus 54.2±28.1; $p<0.05$) post-IRI (Fig. 2C).

MMP-9 inhibition Protected Endothelial PECAM Expression in Steatotic Liver IRI

PECAM-1 expression was readily detected on the intact vascular endothelium of naive steatotic MMP-9−/− and MMP-9+/+ livers. However, while PECAM-1 expression was relatively preserved on the vascular endothelium of MaS-MMP-9−/− livers post-IRI, it was largely absent from the vasculature of control MMP-9+/+ fatty livers, particularly at 6h, after reperfusion (Fig 2D). Double staining of PECAM-1 and vWF factor, a widely accepted endothelial cell marker, showed strong colocalization of both molecules in MaS-MMP-9−/− steatotic livers, whilst PECAM-1 expression was almost absent in the vWF-positive endothelium of MMP-9+/+ fatty livers post-reperfusion (Fig. 2D). Furthermore, the full length PECAM-1 (130 kDa), which was highly detected in naïve livers, it was fairly detected in MaS-MMP-9−/− livers and markedly depressed in MaS-MMP-9+/+ livers (~2.5-fold decrease; $p<0.05$) post-IRI (Fig. 2E). Conversely, a lower molecular mass fragment of about 70-80 kDa, which was minimally expressed in naïve steatotic livers and in MaS-MMP-9−/− livers post-IRI, was eagerly detected in MaS-MMP-9+/+ livers after reperfusion (Fig 2E). The ratio 70-80 kDa/130kDa PECAM-1 was increased by about 4-fold ($p<0.05$) in MaS-MMP-9+/+ livers, compared to MaS-MMP-9−/− livers post-IRI, supporting PECAM-1 cleavage in the presence of MMP-9.

MMP-9 inhibition impaired PECAM-1 cleavage and disrupted leukocyte migration across PECAM-1

To test whether neutrophil-derived MMP-9 is capable of cleaving PECAM-1, we carried out a series of *in vitro* studies using the recombinant extracellular domain of PECAM-1 (rPECAM-1; 100 kDa). The incubation of rPECAM-1 in conditioned medium from fMLP-stimulated WT-neutrophils induced the appearance of PECAM fragments with approximately 80kDa and 20kDa. Indeed, the incubation of rPECAM-1 in the MMP-9-rich medium from the stimulated WT-neutrophils resulted in a several fold increase of the 80 kDa/100kDa (~15-fold increase, $p<0.05$) and 20kDa/100kDa (~9-fold increase, $p<0.05$) PECAM-1 ratios, when compared to incubation of rPECAM-1 in saline (Fig. 3A and B). In contrast, PECAM-1 cleavage was significantly reduced when the incubation of rPECAM-1 in conditioned medium from fMLP-stimulated WT neutrophils was carried out in the presence of a selective MMP-9 inhibitor (80kDa/130kDa:~2-fold decrease, $p<0.05$; 20kDa/

130kDa:~5-fold decrease, $p<0.05$) or when rPECAM-1 was incubated in conditioned medium from fMLP-stimulated MMP-9−/− neutrophils (80kDa/130kDa:~11-fold decrease, $p<0.05$; 20kDa/130kDa:~8-fold decrease, $p<0.05$). Transmigration of CXCL-8-stimulated leukocytes across an endothelial cell monolayer was significantly ($p<0.05$) decreased in the presence of the MMP-9 inhibitor-I (Supplementary Fig. 3C). Furthermore, MMP-9 inhibition significantly ($p<0.05$) reduced the migration of CXCL-8-stimulated neutrophils and TNF-α-activated macrophages particularly across rPECAM-1 (Fig. 3D, and E). MMP-9 inhibition didn't affect leukocyte migration in the uncoated control invasion chambers as leukocytes passed, in the same numbers, unimpeded through the 3-μm pores, as previously shown.[14] These data provide evidence that MMP-9 selective inhibition shelters PECAM-1 from proteolytic processing.

MMP-9 Deficiency Facilitated Hepatocyte Proliferation in Steatotic Liver IRI

Impaired liver regeneration is often attributed to fatty livers.[3] We evaluated the levels of PCNA and phosphorylated histone H3 (p-H3) in MaS-MMP-9−/− livers and respective controls after IRI. MaS-MMP-9−/− livers were characterized by significantly ($p<0.05$) enhanced PCNA (24h:~3-fold increase; 48h:~3-fold increase) and p-H3 (24h:~13-fold increase; 48h:~2-fold increase) expressions when compared to fatty controls (Fig. 4A). MaS-MMP-9−/− livers had markedly increased percentage of cells in S phase, the PCNA labeling index (24h:50±20 versus 15±9; 48h:40±11 versus 24±4; $p<0.05$), and phospho-H3-labeled cells, the mitotic index (MI) (24h:68±7 versus 17±4; 48h:57±8 versus 32±13; $p<0.05$) post-IRI (Fig. 4B and C). Furthermore, as shown in Figure 4C, p-H3 was detected in polygonal cells with the typical hepatocyte morphology. These results show that MMP-9 deficiency accelerated the regeneration of steatotic livers post-IRI.

DISCUSSION

Obesity is a widespread problem in modern societies.[19] Hepatic steatosis, a major complication of obesity, is associated with a higher risk of postoperative morbidity and mortality after surgery.[3] Indeed, the decision of transplant or not to transplant a liver is frequently based on its steatotic characteristics during procurement.[20] We have established a mouse model of steatotic liver IRI, in which mice fed with a high-fat diet developed steatotic livers resembling human obesity;[18] these mice showed approximately 50% liver steatosis, with macrovesicular fat inclusions, after an eight-week feeding period. Moreover, livers with macrovesicular inclusions showed significantly lower tolerance to hepatic ischemia followed by reperfusion, when compared to livers with predominant microvesicular steatosis, consistent with previous observations.[6]

MMP-9 deficiency did not interfere with the ability of mice to develop steatosis. Nevertheless, loss of MMP-9 activity significantly protected steatotic mice from liver IRI; MMP-9−/− steatotic livers showed improved liver function and histological preservation post-IRI. MMP-9-specific gelatinase activity was profoundly upregulated in the extensively necrotic steatotic wild-type livers, consistently with their increased susceptibility to IRI.[21]

The recruitment of activated inflammatory leukocytes into liver plays essential roles in the progression of tissue damage.[7] MMP-9 deficiency markedly depressed the infiltration of

Ly-6G, CD68, and CD3 leukocytes in periportal areas of steatotic livers post-IRI. Overall, these results are in line with the growing number of reports supporting key roles for MMP-9 on leukocyte recruitment into inflamed tissues.[7-9, 11, 14, 22-24]

Increased vascular permeability resulting from impaired endothelial barrier function, is an important feature of hypoxia and ischemia.[25] In addition to promoting ECM breakdown, MMPs can also increase vascular permeability by cleaving junctional proteins.[26] PECAM-1 is a major constituent of the endothelial cell intercellular junctions,[27] and its loss is often regarded as a marker of sinusoidal injury.[28, 29] PECAM-1 expression was readily detected on the vasculature of naïve steatotic livers; however, while PECAM-1 expression was preserved in MaS-MMP-9−/− livers after IRI, its expression was profoundly depressed in MaS-MMP-9+/+ livers post-reperfusion. These observations are supported by our *in vitro* data showing that specific inhibition of neutrophil-derived MMP-9 protected the extracellular portion of PECAM-1 from proteolytic processing, and disrupted leukocyte migration across this junctional molecule. Notably, adenosine triphosphate (ATP), which is released in the extracellular environment in response to a variety of stimuli, promotes tissue inflammation, whereas its conversion to adenosine is cytoprotective in hepatic IRI.[25, 30, 31] It has been demonstrated that ATP induces the release of MMP-9 from leukocytes [24], but adenosine inhibits its secretion.[32] One can postulate that conversion of extracellular ATP to adenosine may in part contribute to hamper MMP-9 mediated cleavage of PECAM-1. The mechanisms by which PECAM-1 modulates vascular integrity and permeability[33] have been linked to its homophilic PECAM-1/PECAM-1 interactions.[34] Indeed, loss of PECAM-1 renders mice more susceptible to vascular leakage/leukocyte accumulation in response to inflammatory stimuli,[35-39] and increases the risk of steatohepatitis associated with liver injury.[38] Considered together, these observations support the view that MMP-9 affects vascular integrity through its ability to promote PECAM-1 proteolytic breakdown in steatotic livers after IRI.

Preservation of vascular endothelial cell barrier integrity in MaS-MMP-9−/− livers may have facilitated their regeneration as intact sinusoidal endothelial cells are required to stimulate the initial burst of hepatocyte proliferation.[40] We show that hepatocyte progression into S phase and mitosis was increased in MMP-9-deficient steatotic livers post-IRI. The mechanisms of liver regeneration are dependent on the nature/extent of tissue injury. For example, the origin of the cells that replace missing hepatocytes differs after partial hepatectomy and parenchymal cell necrosis.[41] Findings that physiologic doses of IL-6 induce liver regeneration, while IL-6 hyperstimulation inhibits the cell cycle progression after partial hepatectomy,[42] provide another example that mechanisms of liver regeneration cannot be generalized. The reduced IL-6 levels in the MMP-9−/− steatotic mice are likely enough to account for its potential pro-regenerative properties. Conversely, overproduction of IL-6, and/or of other proinflammatory factors, in the MaS-MMP-9+/+ livers, may have contributed to their relatively delayed hepatic regeneration. Elevated levels of IL-6 and TNF-α have been detected in livers of patients with fatty liver disease, and inhibition of these cytokines appears beneficial in experimental models of fatty liver disorders.[2] The mechanisms by which MMPs affect liver regeneration are likely multifactorial. MMP-mediated shedding of c-met tyrosine kinase (cMet), the hepatocyte

growth factor receptor, may have also contributed to the impaired liver regeneration of steatotic livers in settings of high MMP-9 activity.[15] Further experimentation is needed to better understand the intricate MMP-dependent mechanisms that underlie hepatic regeneration following an IR-insult.

Here we demonstrate that the inability of MMP-9−/− steatotic mice to express MMP-9 protected these mice from liver IRI. MMP-9−/− deficient fatty livers were characterized by decreased leukocyte infiltration/activation, reduced necrosis, and enhanced hepatocyte proliferation after IRI. Loss of MMP-9 preserved the endothelial expression of PECAM-1, a key modulator of vascular integrity. Using in vitro culture systems, we show that specific inhibition of neutrophil-derived MMP-9 sheltered the extracellular domain of PECAM-1 from proteolytic degradation, and disrupted cell migration across this molecule. Overall, we provide evidence that MMP-9 targeted therapies would allow more patients to undergo successful liver transplantation by IRI.

Supplementary Material

Refer to Web version on PubMed Central for supplementary material.

Acknowledgments

Financial Support: This work was supported by grants from the National Institutes of Health (NIH), National Institute of Allergy and Infectious Diseases (NIAID) R01AI057832 and the Pfleger Foundation.

List of Abbreviations

ALT	alanine aminotransferase
AST	aspartate aminotransferase
ECM	extracellular matrix
M/MMP-9−	conditioned medium from fMLP-stimulated MMP-9−/− neutrophils
M/MMP-9+	conditioned medium from fMLP-stimulated MMP-9+/+ neutrophils
HFD	high-fat diet
pH3	histone H3 phosphorylation
IRI	ischemia and reperfusion injury
MaS	macrovesicular steatosis
MMP	matrix metalloproteinase
MiS	microvesicular steatosis
PECAM-1	platelet endothelial cell adhesion molecule-1
PCNA	proliferating cell nuclear antigen
vWF	von Willebrand factor
WT	wild-type

REFERENCES

1. de Rougemont O, Dutkowski P, Clavien PA. Biological modulation of liver ischemia-reperfusion injury. Curr Opin Organ Transplant. 2010; 15:183–9. [PubMed: 20125019]
2. Cohen JC, Horton JD, Hobbs HH. Human fatty liver disease: old questions and new insights. Science. 2011; 332:1519–23. [PubMed: 21700865]
3. Selzner M, Clavien PA. Fatty liver in liver transplantation and surgery. Semin Liver Dis. 2001; 21:105–13. [PubMed: 11296690]
4. Verran D, Kusyk T, Painter D, et al. Clinical experience gained from the use of 120 steatotic donor livers for orthotopic liver transplantation. Liver Transpl. 2003; 9:500–5. [PubMed: 12740794]
5. Marsman WA, Wiesner RH, Rodriguez L, et al. Use of fatty donor liver is associated with diminished early patient and graft survival. Transplantation. 1996; 62:1246–51. [PubMed: 8932265]
6. Selzner N, Selzner M, Jochum W, et al. Mouse livers with macrosteatosis are more susceptible to normothermic ischemic injury than those with microsteatosis. J Hepatol. 2006; 44:694–701. [PubMed: 16229921]
7. Coito AJ. Leukocyte transmigration across endothelial and extracellular matrix protein barriers in liver ischemia/reperfusion injury. Curr Opin Organ Transplant. 2011; 16:34–40. [PubMed: 21150609]
8. Sato W, Tomita A, Ichikawa D, et al. CR2(+)CCR5(+) T cells produce matrix metalloproteinase-9 and osteopontin in the pathogenesis of multiple sclerosis. J Immunol. 2012; 189:5057–65. [PubMed: 23071279]
9. Moore BA, Manthey CL, Johnson DL, Bauer AJ. Matrix metalloproteinase-9 inhibition reduces inflammation and improves motility in murine models of postoperative ileus. Gastroenterology. 2011; 141:1283–92. 1292 e1-4. [PubMed: 21703213]
10. Lee SY, Horbelt M, Mang HE, et al. MMP-9 gene deletion mitigates microvascular loss in a model of ischemic acute kidney injury. Am J Physiol Renal Physiol. 2011; 301:F101–9. [PubMed: 21454251]
11. Lingwal N, Padmasekar M, Samikannu B, et al. Inhibition of gelatinase B (matrix metalloprotease-9) activity reduces cellular inflammation and restores function of transplanted pancreatic islets. Diabetes. 2012; 61:2045–53. [PubMed: 22586582]
12. Ma ZY, Qian JM, Rui XH, et al. Inhibition of matrix metalloproteinase-9 attenuates acute small-for-size liver graft injury in rats. Am J Transplant. 2010; 10:784–95. [PubMed: 20121733]
13. Moore C, Shen XD, Gao F, et al. Fibronectin-alpha4beta1 integrin interactions regulate metalloproteinase-9 expression in steatotic liver ischemia and reperfusion injury. Am J Pathol. 2007; 170:567–77. [PubMed: 17255325]
14. Hamada T, Fondevila C, Busuttil RW, Coito AJ. Metalloproteinase-9 deficiency protects against hepatic ischemia/reperfusion injury. Hepatology. 2008; 47:186–98. [PubMed: 17880014]
15. Duarte S, Hamada T, Kuriyama N, et al. TIMP-1 deficiency leads to lethal partial hepatic ischemia and reperfusion injury. Hepatology. 2012; 56:1074–85. [PubMed: 22407827]
16. Duarte S, Shen XD, Fondevila C, et al. Fibronectin-alpha4beta1 interactions in hepatic cold ischemia and reperfusion injury: regulation of MMP-9 and MT1-MMP via the p38 MAPK pathway. Am J Transplant. 2012; 12:2689–99. [PubMed: 22812390]
17. Liu G, Place AT, Chen Z, et al. ICAM-1-activated Src and eNOS signaling increase endothelial cell surface PECAM-1 adhesivity and neutrophil transmigration. Blood. 2012; 120:1942–52. [PubMed: 22806890]
18. Li Z, Soloski MJ, Diehl AM. Dietary factors alter hepatic innate immune system in mice with nonalcoholic fatty liver disease. Hepatology. 2005; 42:880–5. [PubMed: 16175608]
19. Kopelman PG. Obesity as a medical problem. Nature. 2000; 404:635–43. [PubMed: 10766250]
20. Cameron AM, Ghobrial RM, Yersiz H, et al. Optimal utilization of donor grafts with extended criteria: a single-center experience in over 1000 liver transplants. Ann Surg. 2006; 243:748–53. discussion 753-5. [PubMed: 16772778]
21. Selzner M, Rudiger HA, Sindram D, et al. Mechanisms of ischemic injury are different in the steatotic and normal rat liver. Hepatology. 2000; 32:1280–8. [PubMed: 11093735]

22. Gong Y, Hart E, Shchurin A, Hoover-Plow J. Inflammatory macrophage migration requires MMP-9 activation by plasminogen in mice. J Clin Invest. 2008; 118:3012–24. [PubMed: 18677407]
23. Budatha M, Roshanravan S, Zheng Q, et al. Extracellular matrix proteases contribute to progression of pelvic organ prolapse in mice and humans. J Clin Invest. 2011; 121:2048–59. [PubMed: 21519142]
24. Gu BJ, Wiley JS. Rapid ATP-induced release of matrix metalloproteinase 9 is mediated by the P2X7 receptor. Blood. 2006; 107:4946–53. [PubMed: 16514055]
25. Eltzschig HK, Eckle T. Ischemia and reperfusion--from mechanism to translation. Nat Med. 2011; 17:1391–401. [PubMed: 22064429]
26. Reijerkerk A, Kooij G, van der Pol SM, et al. Diapedesis of monocytes is associated with MMP-mediated occludin disappearance in brain endothelial cells. FASEB J. 2006; 20:2550–2. [PubMed: 17065217]
27. Newman PJ. The biology of PECAM-1. J Clin Invest. 1997; 99:3–8. [PubMed: 9011572]
28. Zhao X, Koshiba T, Nakamura T, et al. ET-Kyoto solution plus dibutyryl cyclic adenosine monophosphate is superior to University of Wisconsin solution in rat liver preservation. Cell Transplant. 2008; 17:99–109. [PubMed: 18468240]
29. Ramadori G, Moriconi F, Malik I, Dudas J. Physiology and pathophysiology of liver inflammation, damage and repair. J Physiol Pharmacol. 2008; 59(Suppl 1):107–17. [PubMed: 18802219]
30. Eltzschig HK, Carmeliet P. Hypoxia and inflammation. N Engl J Med. 2011; 364:656–65. [PubMed: 21323543]
31. Zimmerman MA, Grenz A, Tak E, et al. Signaling through hepatocellular A2B adenosine receptors dampens ischemia and reperfusion injury of the liver. Proc Natl Acad Sci U S A. 2013; 110:12012–7. [PubMed: 23812746]
32. Ernens I, Rouy D, Velot E, et al. Adenosine inhibits matrix metalloproteinase-9 secretion by neutrophils: implication of A2a receptor and cAMP/PKA/Ca2+ pathway. Circ Res. 2006; 99:590–7. [PubMed: 16917093]
33. Ilan N, Madri JA. PECAM-1: old friend, new partners. Curr Opin Cell Biol. 2003; 15:515–24. [PubMed: 14519385]
34. Privratsky JR, Paddock CM, Florey O, et al. Relative contribution of PECAM-1 adhesion and signaling to the maintenance of vascular integrity. J Cell Sci. 2011; 124:1477–85. [PubMed: 21486942]
35. Graesser D, Solowiej A, Bruckner M, et al. Altered vascular permeability and early onset of experimental autoimmune encephalomyelitis in PECAM-1-deficient mice. J Clin Invest. 2002; 109:383–92. [PubMed: 11827998]
36. Tada Y, Koarada S, Morito F, et al. Acceleration of the onset of collagen-induced arthritis by a deficiency of platelet endothelial cell adhesion molecule 1. Arthritis Rheum. 2003; 48:3280–90. [PubMed: 14613294]
37. Maas M, Stapleton M, Bergom C, et al. Endothelial cell PECAM-1 confers protection against endotoxic shock. Am J Physiol Heart Circ Physiol. 2005; 288:H159–64. [PubMed: 15319204]
38. Goel R, Boylan B, Gruman L, et al. The proinflammatory phenotype of PECAM-1-deficient mice results in atherogenic diet-induced steatohepatitis. Am J Physiol Gastrointest Liver Physiol. 2007; 293:G1205–14. [PubMed: 17932230]
39. Privratsky JR, Tilkens SB, Newman DK, Newman PJ. PECAM-1 dampens cytokine levels during LPS-induced endotoxemia by regulating leukocyte trafficking. Life Sci. 2012; 90:177–84. [PubMed: 22119535]
40. Ding BS, Nolan DJ, Butler JM, et al. Inductive angiocrine signals from sinusoidal endothelium are required for liver regeneration. Nature. 2010; 468:310–5. [PubMed: 21068842]
41. Fausto N, Campbell JS, Riehle KJ. Liver regeneration. Hepatology. 2006; 43:S45–53. [PubMed: 16447274]
42. Wustefeld T, Rakemann T, Kubicka S, et al. Hyperstimulation with interleukin 6 inhibits cell cycle progression after hepatectomy in mice. Hepatology. 2000; 32:514–22. [PubMed: 10960443]

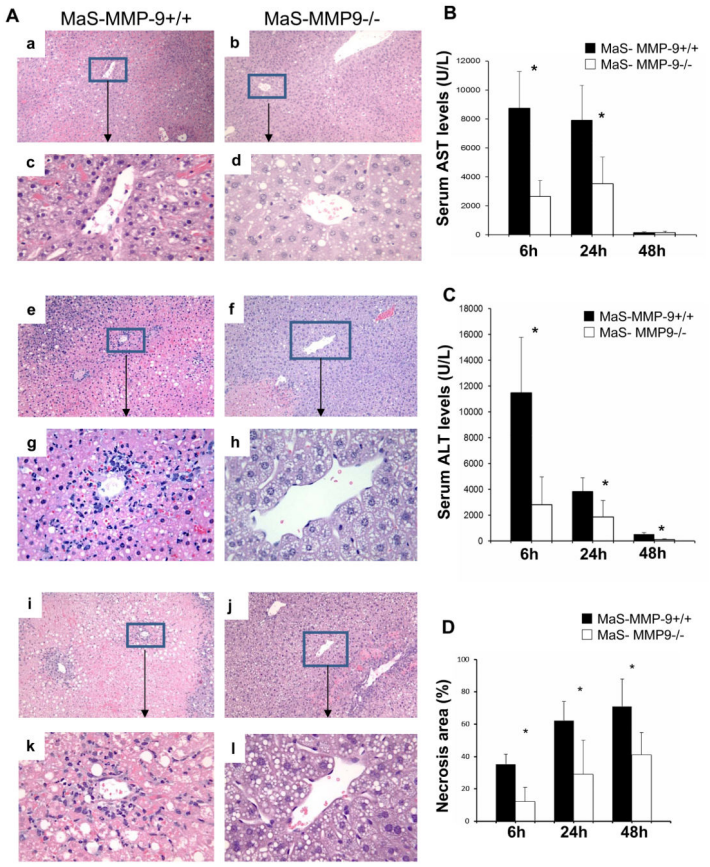

Figure 1.

Liver histology and serum transaminases in MaS-MMP-9−/− (white bars) and MaS-WT (black bars) mice. H&E staining (panel A) of MaS-MMP-9+/+ (a, c, e, g, i, and k) and MaS-MMP-9−/− (b, d, f, h, j, and l) livers evidence that MMP-9 deficiency resulted in a significant improvement of liver histological preservation at 6h (a-d), 24h (e-h) and 48h (i-l) post-IRI. sAST (panel B) and sALT (panel C) levels were significantly decreased in MaS-MMP-9−/− mice, when compared with controls. The percentage of hepatocellular necrosis (panel D) was decreased in the MaS-MMP-9−/− livers post-IRI. (n=4-6 mice/group *$p<0.05$).

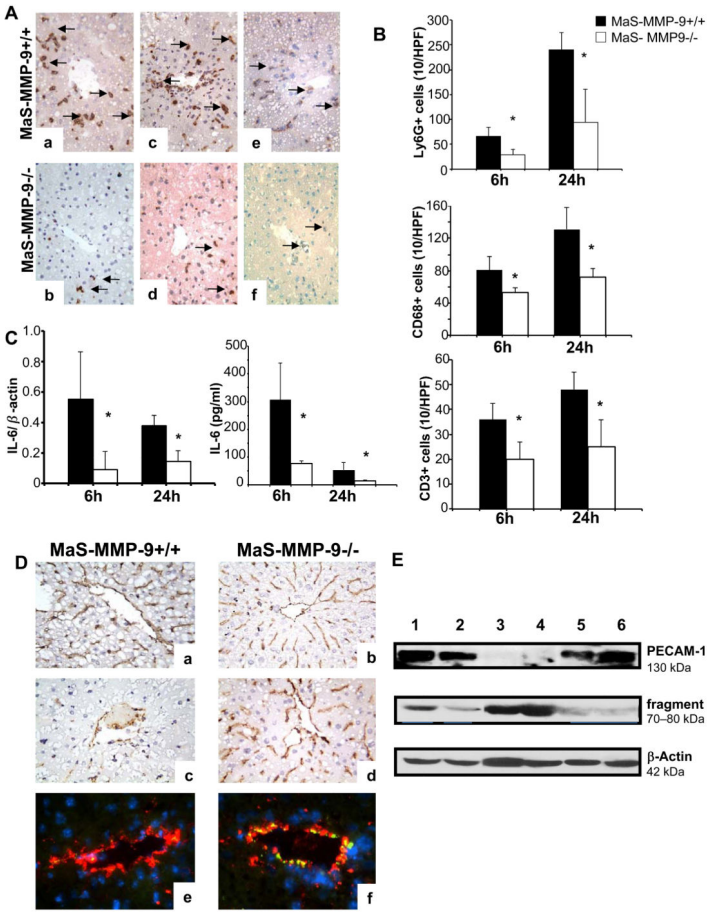

Figure 2.

Leukocyte infiltration/activation and PECAM expression in MaS-MMP-9−/− (white bars) and MaS-WT (black bars) mice. Ly-6G+ neutrophil (a, and b), CD68+ macrophage (c, and d), and CD3 lymphocyte (e, and f) staining in MaS-MMP-9+/+ (a, c, and e) and MaS-MMP-9−/− (b, d, and f) livers at 6h post-reperfusion (panel A). Infiltrating leukocytes (panel B), and IL-6 liver mRNA/serum protein levels (panel C) were depressed in MaS-MMP-9−/− mice when compared with respective controls at 6h and 24h post-IRI. PECAM-1 staining (panel D) was readily detected in MaS-MMP-9+/+ (a) and MaS-MMP-9−/− (b) naïve livers, and in MaS-MMP-9−/− livers (d, and f) 6h post-reperfusion; PECAM-1 was markedly depressed in MaS-MMP-9+/+ control livers (c, and e); staining overlay of PECAM-1 in green (Alexa Fluor 488 phalloidin), vWF in red (Alexa Fluor 594), and nuclear stain in blue (Dapi) (e,f). Western blotting of PECAM-1 (panel E) shows the intact 130 kDa-PECAM-1 form readily expressed in naïve Mas-MMP-9+/+ livers (lane 1), naïve MaS-MMP-9−/− livers (lane 2), and in MaS-MMP-9−/− livers at 6h post-IRI (lanes 5, and 6), and minimally detected in MaS-MMP-9+/+ livers after 6h of reperfusion (lanes 3, and 4). The anti-PECAM-1 antibody reacted also with an additional fragment of about 70-80 kDa, predominantly detected in the Mas-MMP-9+/+ livers (lanes 3, and 4) post-IRI (n=5-6/group; *p<0.05).

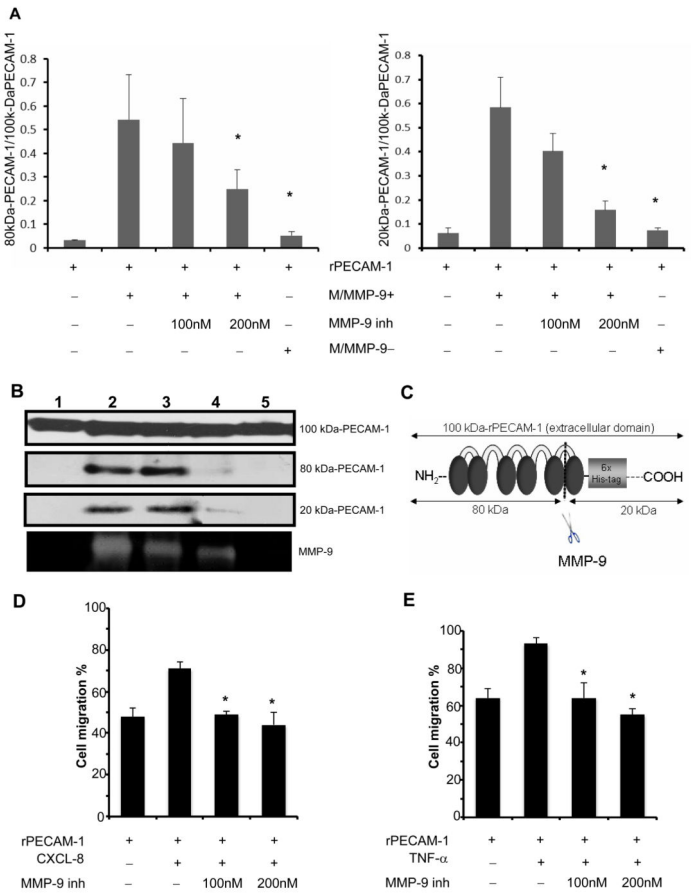

Figure 3.

Cleavage of PECAM-1 by neutrophil-derived MMP-9. In panel A, the incubation of the recombinant extracellular domain of PECAM-1 (rPECAM-1; 100 kDa) in MMP-9-rich medium (M/MMP-9+) from the stimulated WT-neutrophils resulted in a profound increase of the 80 kDa/100kDa and 20 kDa/100kDa PECAM-1 ratios, compared with incubation in saline. PECAM-1 cleavage was reduced when the incubation of rPECAM-1 in conditioned medium from fMLP-stimulated WT neutrophils (M/MMP-9+) was carried out in the presence of a selective MMP-9 inhibitor (MMP-9 inh-200nM) or when rPECAM-1 was incubated in conditioned medium from fMLP-stimulated MMP-9−/− neutrophils (M/MMP-9−). The different size forms of PECAM-1 (panel B) resulting from the incubation of rPECAM-1 in saline (lane 1), MMP-9-rich medium (M/MMP-9+) (lane 2), MMP-9-rich medium (M/MMP-9+) with MMP-9 inh 100nM (3), MMP-9-rich medium (M/MMP-9+) with MMP-9 inh 200nM (4), and in MMP-9-negative medium (M/MMP-9−). The MMP-9 activity correspondent to the different culture combinations is shown at the bottom. The schematic representation of rPECAM-1 and its fragments after MMP-9 cleavage (panel C). Migration of neutrophils (panel D) and macrophages (panel E) across PECAM-1 was impaired in the presence of a MMP-9 specific inhibitor (data expressed as mean ± SD of three independent experiments; *p< 0.05).

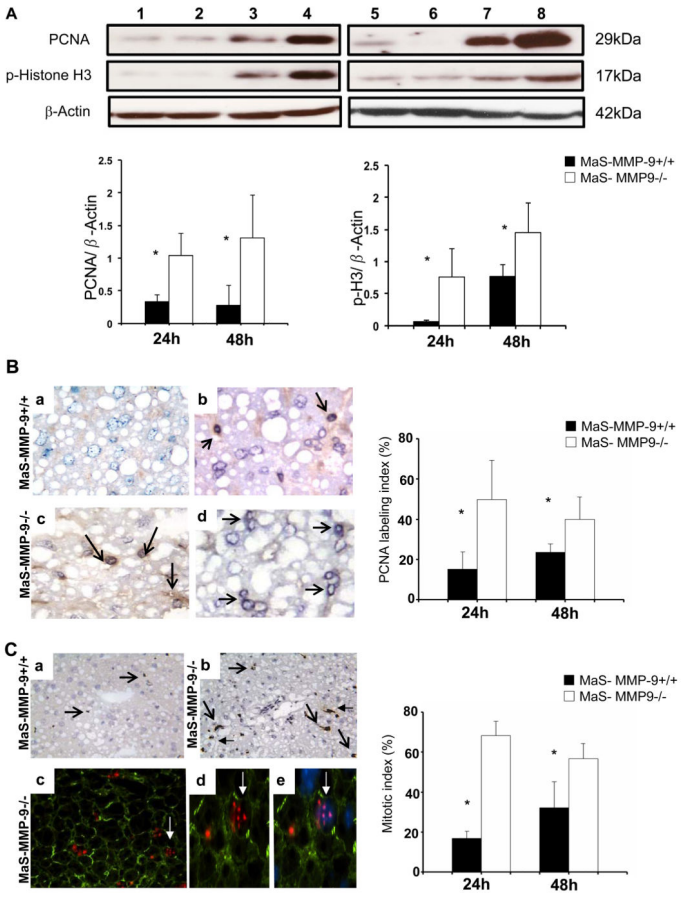

Figure 4.

Expression of hepatic regenerative markers in Mas-MMP-9−/− (white bars) and MaS-MMP-9+/+ (black bars) mice. PCNA and phosphorylated histone H3 (panel A) expressions were upregulated in MaS-MMP-9−/− livers (lanes 3, 4, 7, and 8), compared with MaS-WT controls (lanes 1, 2, 5, and 6) at 24h (lanes 1-4) and 48h (lanes 5-8) post-IRI. PCNA labeling (panel B) in Mas-MMP-9−/− (c, and d) and MaS-MMP-9+/+ (a, and b) livers at 24h (a, and c) and 48h (b, and d) post-IRI. Phosphorylated histone H3-positive cells (panel C) in Mas-MMP-9−/− (b, c, d, and e) and MaS-MMP-9+/+ (a) livers at 48 post-IRI; pH3 in red (c,d, and e; Alexa Fluor 594), F-actin in green (c,d, e; Alexa Fluor 488 phalloidin), nuclear stain in blue (e; Dapi) staining overlay. MaS-MMP-9−/− livers showed significantly increased PCNA, and mitotic labeling indexes at 24h and 48h post-IRI, when compared with controls (n=4-5/group; *p<0.05).

Table 1

Basic characteristics of MMP−9−/− and MMP−9+/+ MaS mice after 8 weeks of HFD

Characteristics	MMP−9+/+	MMP−9−/−	Significance
Body weight (g)	39.0 ± 2.7	37.7 ± 3.3	n.s
Liver weight (g)	1.3 ± 0.2	1.2 ± 0.1	n.s.
Liver/body weight (%)	3.6 ± 0.3	3.4 ± 0.2	n.s.
Triglycerides (μg/mg liver)	99.9 ± 23	97.8 ± 16	n.s.
Liver fat (% Oil Red−0)	46.5 ± 6.9	45.3 ± 5.8	n.s.

n.s., not significant